MAGNETIC FIELDS AND CORONAL STRUCTURES

E. R. Priest

Mathematical and Computational Sciences Dept., St Andrews University, St Andrews KY16 9SS, Scotland

ABSTRACT

One of the main aims of SOHO is to try and determine how the solar corona is heated. Here we first of all propose answers to the questions: why do some loops have a higher pressure than others and how are they contained? Then we summarise the main theories that have been proposed to heat the corona by waves, by reconnection in current sheets or by MHD turbulence, and in particular give some new results on the signature of braiding. Advances in solving the coronal heating problem are described, including the realisations that: most x-ray bright points are heated by driven reconnection (the converging flux model); Yohkoh observations suggest that loops are heated by two distinct mechanisms, namely an impulsive mechanism (probably reconnection) and a steadier background mechanism. Finally, a new technique is proposed for identifying the form of the heating mechanism, namely comparing observations of the temperature structure with loop models having different heating forms. This is a spur to theorists to deduce the form of heating produced by different models and to observers to determine temperature profiles with high accuracy. Applied to the large-scale diffuse corona as observed by Yohkoh, this technique implies that the heating is likely to be uniformly distributed along a loop: unless Alfvén waves can heat uniformly, the evidence is therefore in favour of turbulent microflare heating.

Key words: magnetic fields, corona, reconnection.

1. INTRODUCTION

The solar corona is incredibly beautiful and complex; and it is the magnetic field that creates its three-fold structure of coronal holes, coronal loops and x-ray bright points. Today I plan: to discuss the structure of coronal loops (Section 2); to give a brief review of theories of coronal heating, either by waves, current sheets or turbulence (Section 3); to describe the recent advances in solving parts of the coronal heating problem (Section 4); and to suggest a new technique for deducing the form of the coronal heating mechanism (Section 5). I shall not aim to summarise what we have learnt so far from SOHO, since that is being done by the PI's in their reviews and in the working groups. Rather, I plan to try and give a general background to the physical processes at work as a preparation for our future SOHO studies.

From Skylab we deduced temperatures for x-ray bright points of 1.3 - 1.7 MK, coronal holes of 1.4 - 1.8 MK, active-region coronal loops of 2.2 - 2.8 MK, quiet-region loops of 1.5 - 2.1 MK and interconnecting loops of 2MK. Clearly, these and the other parameters need to be reassessed in the light of Yohkoh and SOHO and, in particular, much higher temperatures are sometimes found.

Many coronal structures are in equilibrium under a balance

$$\mathbf{j} \times \mathbf{B} - \nabla p + \rho \mathbf{g} = 0 \qquad (1)$$

between a magnetic force, a pressure gradient and gravity, where $\mathbf{j} = \nabla \times \mathbf{B}/\mu$ and the magnetic force can be written as the sum of a magnetic pressure force $(-\nabla(B^2/(2\mu))$ and a magnetic tension force $((\mathbf{B} \cdot \nabla)\mathbf{B}/\mu)$. The ratio of the second to the first term in (1) is the plasma beta

$$\beta \equiv \frac{P}{B^2/(2\mu)} = 3.5 \times 10^{-21} \frac{nT}{B^2} \qquad (2)$$

and so is about 10^{-3} for $n = 10^{15} m^{-3}, T = 2 \times 10^6$K, B= 100G. The ratio of the third to the second term is

$$\delta = \frac{\Lambda}{h}, \qquad (3)$$

where $\Lambda = p/(\rho g) \approx 50$ T metres is the scale height (roughly 100 Mm for $T = 2 \times 10^6$K) and h is the height of the structure. In the corona usually the flow speed (v) is much less than the Alfvén speed (v_A) (so we are justified in neglecting the inertial term in (1) and also $\beta \ll 1, \beta\delta \ll 1$, so that ($c$) reduces to a force-free balance

$$(\nabla \times \mathbf{B}) \times \mathbf{B} = 0, \qquad (4)$$

which may be solved to produce magnetic models for loops and arcades. The exceptions are for highly dynamic phenomena (where $v \approx v_A$), in weak-field regions (where the pressure gradient is important) and in large structures or prominences (where $\delta \approx 1$).

The coronal magnetic field lines are anchored in the dense photosphere (where $\beta \geq 1$) and their footpoints are carried around by a variety of surface motions (on a timescale τ). The corona then evolves in a way that may be described as wave-like if the footpoint timescale is less than about ten times the Alfvén

Proceedings of the Fifth SOHO Workshop, 'The Corona and Solar Wind near Minimum Activity', Oslo, Norway, 17-20 June 1997 (ESA SP-404, September 1997)

travel time along a loop of length $2L$ ($\tau < 10L/v_A$), whereas it is a slow evolution through a series of equilibria if $\tau > 10L/v_A$. The energy is injected from the photosphere as a Poynting flux

$$\mathbf{S} \equiv \mathbf{E} \times \mathbf{B}/\mu = -(\mathbf{v} \times \mathbf{B}) \times \mathbf{B}/\mu = v_x B_z B_x/\mu \quad (5)$$

when the footpoint field has vertical and horizontal components B_z and B_x and is moved by a velocity v_x, say. Thus if v_x and B_z are given, $\mathbf{S}$ is not imposed but is for many purposes determined by the coronal evolution (which gives B_x at the base).

Now what happens to the energy that is injected through the solar surface (S)? The answer is given by Poynting's theorem

$$\int_S \mathbf{E} \times \mathbf{H} \cdot \mathbf{dS} = \int_V \frac{j^2}{\sigma} dV + \frac{\partial}{\partial t} \int_V \frac{B^2}{2\mu} dV + \int \mathbf{v} \cdot \mathbf{j} \times \mathbf{B} dV \quad (6)$$

which states that the inflow of electromagnetic energy through the solar surface produces ohmic heating, a rise in magnetic energy and work done by $\mathbf{j} \times \mathbf{B}$. Thus, some energy is continuously dissipated and heats the corona directly (the first term on the right of (6)), whereas some is stored and eventually released as an eruption or flare or microflare and some accelerates the plasma, which may in turn either escape or be dissipated by viscosity or shock waves; the second and third terms in (6) may therefore lead to an indirect heating of the corona.

What is the nature of the coronal plasma? Essentially, it appears to be a dynamic turbulent environment, with a wide range of lows and fine-scale structure (e.g. from EIT, Schriver, at this workshop). There is a general unresolved turbulent value of 10 - 40 km s^{-1} Mason (1991), which is being reassessed by e.g. Brekke (at this workshop). Sometimes one finds explosive events at 250 km s^{-1} (Brueckner, Sarro, Erdelyi, Wilhelm). In addition impulsive events are seen in the ultraviolet in x-rays and in radio (Harrison, Crosby at this workshop).

The heat required to balance radiation, conduction and outflow is about 600 Wm^{-2} for a coronal hole, 300 Wm^{-2} for a quiet region and 5000 Wm^{-2} for an active region, but clearly these values need to be reassessed in the light of SOHO. The heating mechanism is probably magnetic since the acoustic flux is only 10 Wm^{-2} in the transition region, the magnetic regions are hotter, and there is plenty of electromagnetic energy since the Poynting flux is in order of magnitude

$$S \sim \frac{EB}{\mu} \sim \frac{vB^2}{\mu} Wm^{-2} \quad (7)$$

and so this is about 10^4 Wm^{-2} for $v \sim 0.1$ km s^{-1} and $B \sim 100G$.

2. THE STRUCTURE OF CORONAL LOOPS

Skylab and Yohkoh have shown that some loops have a higher plasma pressure than others and that this is often where the magnetic field is larger, such as in active regions. Why do some loops have a higher pressure? Is it because they are twisted? If $\delta \ll 1$ so that the loop height (h) is larger than the scale height (Λ), then

$$\nabla p = \mathbf{j} \times \mathbf{B} \quad (8)$$

and so, taking the scalar product with $\mathbf{B}$,

$$\mathbf{B} \cdot \nabla p = 0 \quad (9)$$

or in other words the plasma pressure (p) is constant along each field line. If, therefore the pressure (p_0) at the coronal base is uniform, i.e. the same at all footpoints, then the pressure will be uniform throughout the arcade (Figure 1a). Starting with a loop of uniform pressure and twisting it up while maintaining a uniform footpoint pressure just produces a force-free loop with a strong magnetic core and having the magnetic tension force in equilibrium everywhere with the

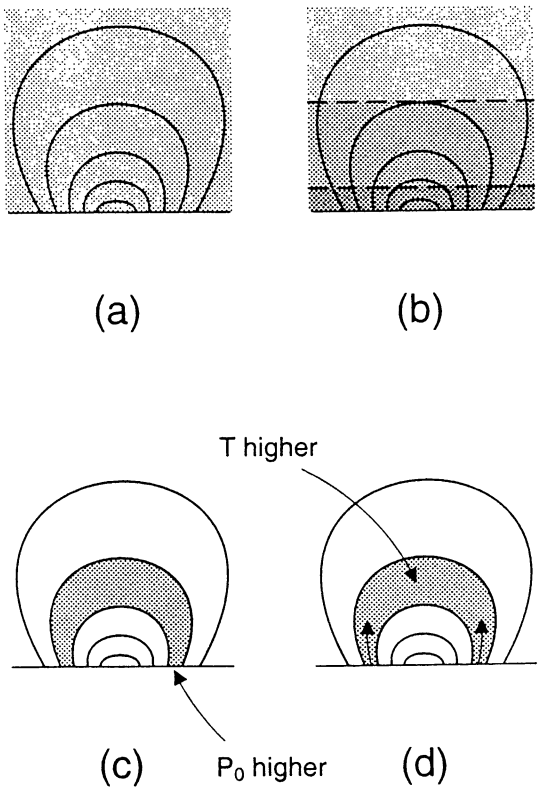

Figure 1. Magnetic arcades having loops with (a) and (b) uniform base pressure, (c) enhanced base pressure (p_0) and (d) enhanced temperature (T)

magnetic pressure force. More generally, if $\delta \geq 1$ so that $h \leq \Lambda$, the component of the force balance (1) along the loop is

$$\nabla p = \rho g \quad (10)$$

and so if the loop temperature is uniform the pressure

$$p = p_0 e^{-z/\Lambda} \quad (11)$$

falls off exponentially with height (z). Thus, if the temperature is uniform throughout the arcade, the

pressure is independent of the structure of the magnetic field and therefore of the twist, since the isobars are simply horizontal (Figure 1b). Our conclusion therefore is that twist cannot by itself create a higher pressure.

So, why do some loops have a higher pressure. One possibility is that the pressure (p_0) at the coronal base of that particular loop is enhanced (Figure 1c), which raises the pressure everywhere along the field line. Another possibility is that the coronal heating is enhanced in that particular loop: if the temperature is higher, then the scale height is longer and so the pressure decreases more slowly with altitude by (11); the resulting excess plasma could be provided by an evaporative upflow from the feet (Figure 1d). A third possiblity is the effect of dynamics (Peres, this workshop) if the flow speeds are very large, i.e. of order the coronal sound speed. It would be useful to test with SOHO which of these possiblities is at work, but to my mind the second seems the most likely.

A second question is that, if a region (such as e.g. an active region) has a higher pressure than its surroundings, then both the plasma pressure gradient and magnetic presure gradient act outwards, so how is it contained? The answer I would suggest is that the magnetic field in a loop with enhanced pressure is slightly lower than it would otherwise be. In a low-beta plasma, small variations in magnetic field can balance large variations in plasma pressure. Thus, for example, consider a potential field arcade with a uniform pressure, in equilibrium everywhere under a balance between a magnetic tension force acting downwards and a magnetic pressure force acting upwards. If you enhance the pressure in one loop of such an arcade, it simply expands slightly (mainly outwards) to a new magnetostatic equilibrium. An example that Longbottom and I have constructed is shown in Figure 2. The initial potential field lines are shown by dashed curves and the final magnetostatic equilibirium by solid curves (Figure 2a). Also shown (Figure 2b) is the profile of magnetic field strength with height along the vertical axis of the arcade. The potential field (solid curve) decreases monotonically. The magnetostatic field is plotted for $\beta = 0.1$ (dotted), $\beta = 0.5$ (dashed), $\beta = 1.0$ (dash-dotted): in the loop it declines with height at first more rapidly and then more slowly than the potential case, even producing a minimum and a maximum when β is large enough; thus the field lines expand in the loop and pile up slightly below, producing a magnetic pressure force to confine the loop both from above and below.

Many groups have constructed linear and nonlinear force-free models of active regions (see e.g. F. Chiuderi, Mikic, at this workshop). A particularly interesting comparison of the nonlinear field computed from a Mees vector magnetogram with Yohkoh active region loops has been made by Jiao et al (1997). They use a relaxation technique with a $90 \times 40 \times 40$ grid and the normal current and magnetic field specified on the lower boundary. Figure 3 shows the computed field lines and the Yohkoh loops with the top line superposing the potential (left) and force-free (right) field lines on the line of sight magnetic field (top row) and current (second row). The force-free field can be seen (in the bottom row) to match the Yohkoh loops much better than the potential field. The main property of the brightest loops is found to be that they

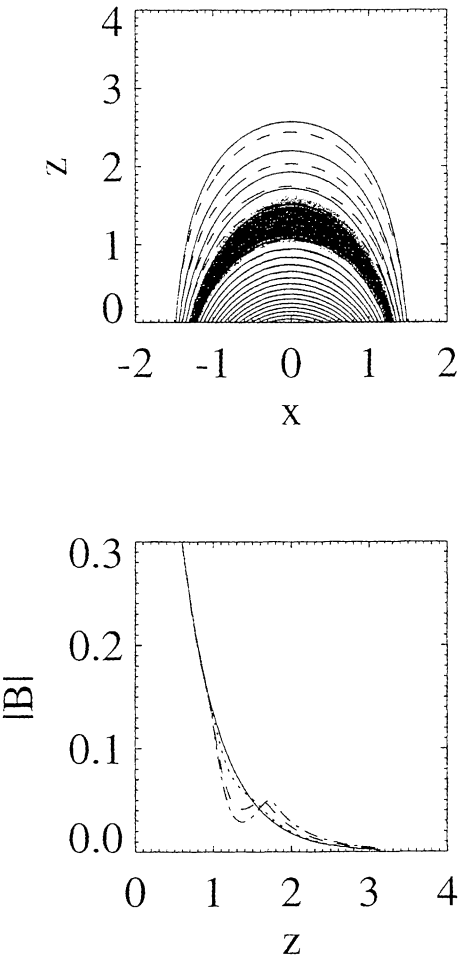

Figure 2. (a) Magnetic structure and (b) magnetic field as a function of height for a potential arcade and one with a loop of enhanced pressure

are rooted in strong fields (about 500G at both feet leading to a summit field of 100 - 250 G). This suggests that the heating is stronger in such loops (see also Sylvester and Sylvester, this workshop).

3. THEORIES FOR CORONAL HEATING

Coronal heating theories may be divided into three classes, namely waves, reconnection and turbulence theories.

3.1. Magnetic Waves

Both Alfvén waves and magnetoacoustic waves are present in general in a magnetic medium, but magnetoacoustic waves are likely to steepen into shocks low down in the atmosphere or become evanescent in the chromosphere and so the emphasis has been on Alfvén waves. Hollweg (1984) recognised that Alfvén waves tend to be reflected at the transition region,

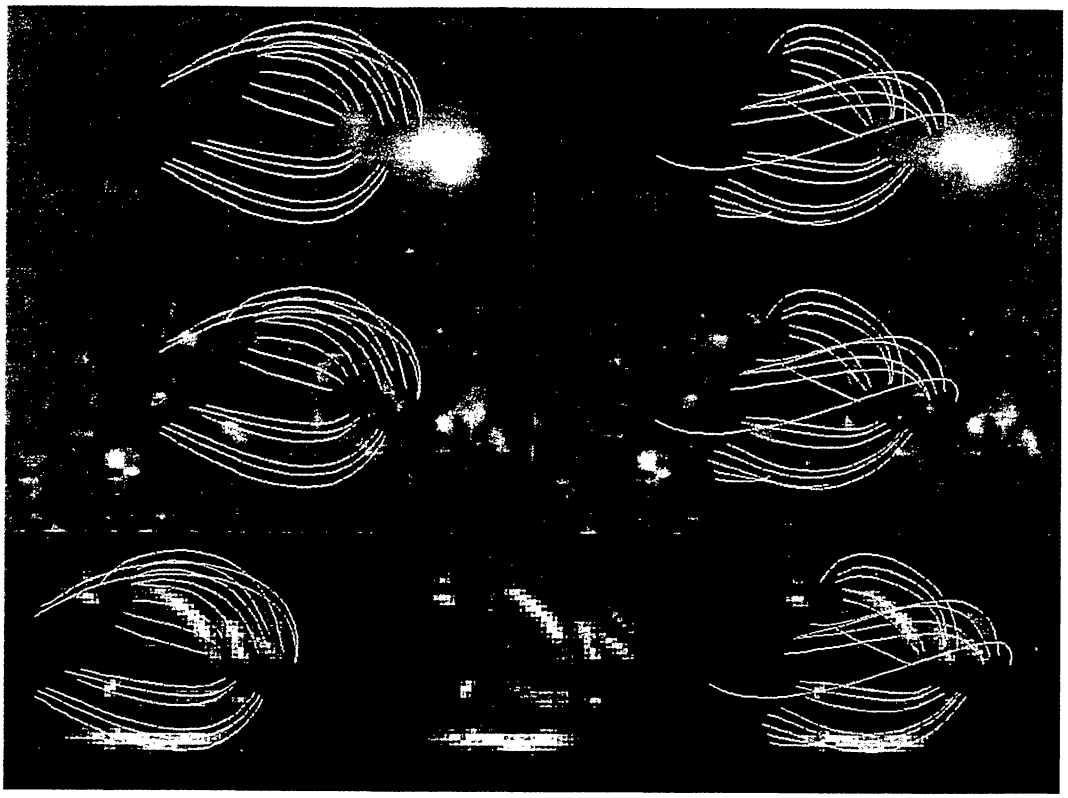

Figure 3. A comparison of potential (left) and force-free (right) fields of an active region with Yohkoh loops (Jiao et al, 1997)

but coronal loops may resonate at discrete frequencies

$$\omega = \frac{nv_A}{2L}, \tag{12}$$

with spatial peaks at distances $\frac{1}{2}, \frac{1}{4}, \frac{3}{4} \ldots$ along the loop. These correspond to periods of typically

$$\tau = \frac{100}{n} \text{ seconds} \tag{13}$$

for a loop length of 100 Mm and Alfvén speed 2000 km s^{-1}, say. The resulting transmission coefficient of waves through into the corona is then enhanced at these resonances. An important question is therefore: can we observe the resonances and spatial peaks with SOHO? If so, it is much more likely for long loops than small ones, since their resonant frequencies are lower and therefore in the part of the spectrum where the photospheric power is high. Possible ways of overcoming the Alfvén wave reflection have been suggested by Velli (this workshop) and Litvin & Rosner (1997). Alfvén waves may dissipate by two effects, the first being phase mixing (Heyvaerts & Priest (1983); Cally (1991); Goossens (1991); Berghmans, this workshop). In a coronal loop, standing waves may be set up which phase mix in time, whereas in a coronal hole propagating waves may phase mix in height. Furthermore, tearing and Kelvin-Helmholtz instabilities may enhance the dissipation (Browning & Priest (1984)). The second effect is resonant absorption (Goedbloed (1975); Goossens (1991); Davila (1987)), which will be discussed extensiviely at this workshop (Berghmans, Erdelyi, Ofman, Belein, Velli, at this workshop). Here the damping rate tends to be independent of resistivity as there is mode conversion and energy accumulation at a resonant surface where the wave frequency matches the Alfvén or cusp frequency.

3.2. Coronal Heating by Magnetic Reconnection in Current Sheets

The idea of heating by nanoflares in many small current sheets has been developed by Parker (1972) and is discussed here by Karlicky, Benz, Judge. First of all, reconnection may occur at null points where the magnetic field vanishes. It is associated with a discontinuity in the mapping of the footpoints as one crosses a separatrix. Slow footpoint motions can drive reconnection at a null, whereas fast motions produce waves that accumulate and dissipate at the null. These processes may occur both in two-dimensional nulls and in the more generic and quite different case (Figure 4a) of three-dimensional nulls (Priest & Titov (1996); Parnell et al (1995); Craig & Fabling (1996)).

However, reconnection can also occur in the absence of nulls (Schindler et al (1988)) at quasi-separatrix layers Priest & Demoulin (1995). When no null is present, the mapping of footpoints from one boundary to another is continuous, but it can have steep enough gradients in thin quasi-separatrix layers that the magnetic field can slip through the plasma (Fig-

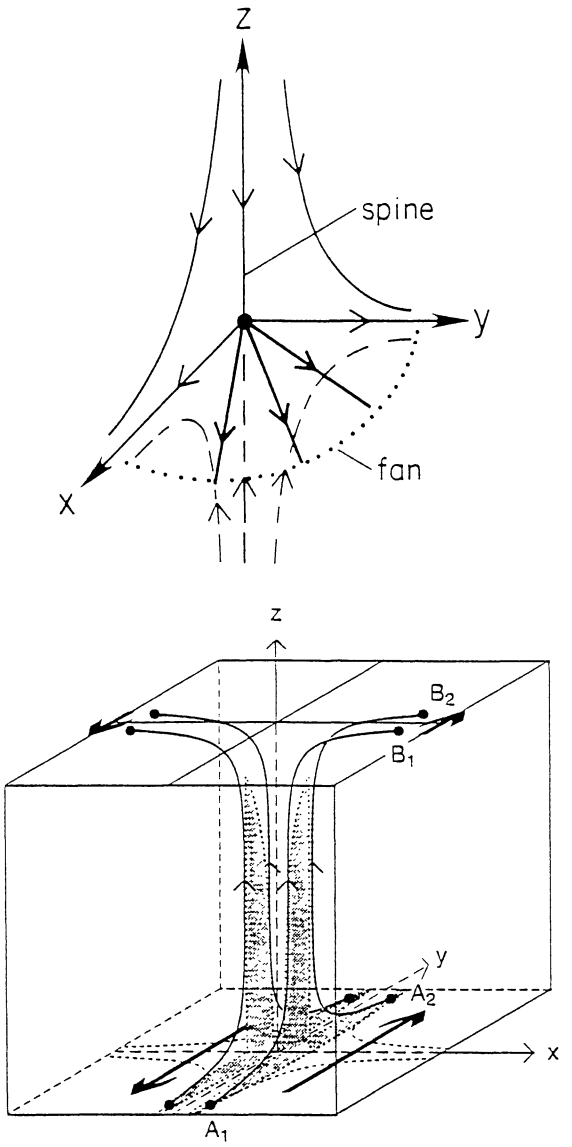

Figure 4. Reconnection in (a) a 3D null and (b) a quasi-separatrix layer

ure 4b) and change the magnetic connectivity of plasma elements - i.e. it reconnects. Indeed small flares have been shown to occur at quasi-separatrix layers (Demoulin et al (1996)).

In addition, reconnection may also occur at current sheets that form in response to slow braiding motions of footpoints (Parker (1972); Van Ballegooijen (1986); Mikic et al (1990)). Recently, Galsgaard & Nordlund (1996), Galsgaard et al (1997) have conducted a 3D resistive MHD numerical experiment with 136^3 points on braiding by applying sinusoidal 3D resistive MHD shear velocities with random amplitude, phase and duration at two boundaries of an initially straight field. The current density in across-section (Figure 5) shows an initial exponential growth of current density and later a transition to a dynamic state with current sheets continually forming and dissipating and super-Alfvénic jets being accelerated. The Poynting flux fluctuates in time (solid curve of Figure 6a) while the Joule dissipation occurs in a series of bursts (dashed curve, Figure 6a). The spatial location of the current sheets depends on the rate of driving (v_d) and the mean time ($< t_d >$) between the random changes in driving relative to the Alfvén time (t_A). For example when the driving is rapid with $< t_d >= t_A$ and $v_d = 0.2 v_A$, you find many small randomly distributed current sheets (Figure 6b), whereas slow driving with $< t_d >= 3 t_A$ and $v_d = 0.02 v_A$ produces a small number of current sheets with large bursty heating events (Figure 6c).

The joule dissipation therefore depends on the rate of driving. Rapid driving (Figure 7a) produces large transients near the feet from the formation of the first current sheet. Later there are many sheets at random locations and an average over time (Figure 7b) gives peaks at both the feet and summit of a loop. Slow driving, on the other hand (Figure 7c) gives two large sheets that change in location and strength. Enhancements of the sheets can be seen as waves propagate across the loop in response to boundary motions. A time-average (Figure 7d) gives a much smaller heating that is much more uniform although it still possesses slight peaks at feet and summit. It will be interesting to see how those results are changed when large-scale curvature in the loop is included.

3.3. Coronal Heating by MHD Turbulence

Braiding or waves often leads to a state of MHD turbulence and so the question arises how one can describe such a state.

Heyvaerts & Priest (1984) were the first to stress the importance of magnetic helicity in the solar corona. They suggested that coronal fields evolve through global force-free fields ($\nabla \times \mathbf{B} = \alpha_0 \mathbf{B}$) with the footpoint connections continually broken and α_0 determined from the evoloution of the magnetic helicity. Conceptually, an arcade may be stressed and energy built up until it goes unstable to small-scale instabilities of many kinds and so it relaxes and reconnects, liberating heat in the process. But this theory was incomplete in the sense that it doesn't give the coronal heating in terms of the photospheric motions alone. So Heyvaerts & Priest (1993), Inverarity et al (1993) developed a new self-consistent approach in which they assumed photospheric motions maintain the corona in a turbulent state with turbulent transport coefficients (ν^* and η^*). First of all, they calculated the global MHD state driven by boundary motions, which gave the heat flux F_H as a function of ν^* and η^*. Then they invoked cascade theories of turbulence to determine the ν^* and η^* that result from that F_H. This general philosophy was applied to an arcade, a flux tube and to wave motions. Recent work on turbulent theories by Georgoulis and Petkaki is reported at this workshop.

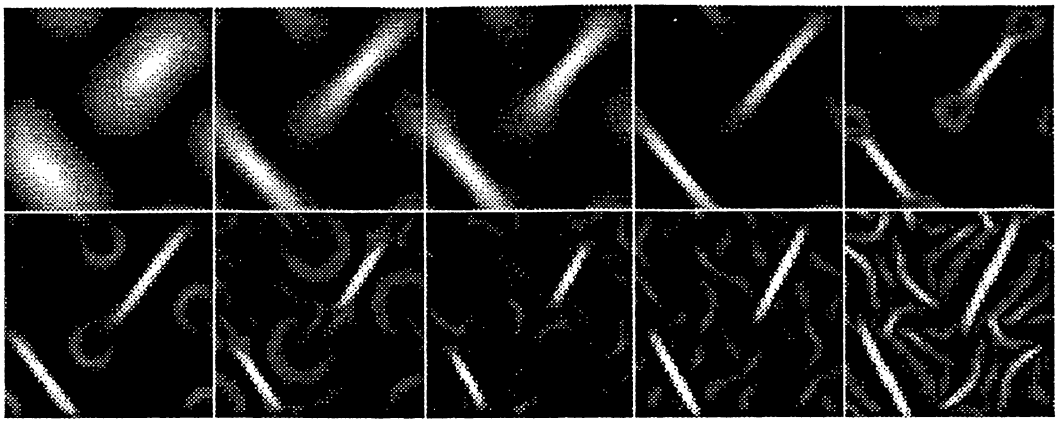

Figure 5. Current density in a braided field (Galsgaard and Nordlund, 1996).

4. THE NEWLY EMERGING PICTURE ABOUT HOW THE CORONA IS HEATED

But, how *is* the corona heated? Which parts of the coronal heating problem have been solved? What is the new picture that is emerging as a background for our future SOHO studies? In particular, let me describe the recent advance in understanding of x-ray bright points and the implications of Yohkoh observations for heating of coronal loops.

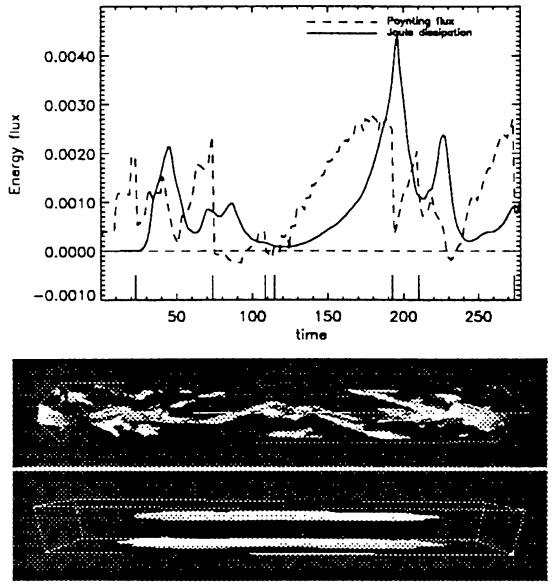

Figure 6. (a) Variation of Poynting flux and Joule dissipation with time. Spatial location of current sheets for (b) fast driving and (c) slow driving.

4.1. X-ray Bright Points

X-ray bright points occur above opposite-polarity magnetic fragments, and Harvey (1985) discovered that about one-third of them are produced by emerging flux but that two-thirds are associated with the cancellation of approaching photospheric magnetic fragments Mason (1991). We therefore proposed a Converging Flux Model Priest et al (1994) to explain the majority case of cancelling flux (Figure 8). In the model, initially the magnetic fragments are connected magnetically and, as they approach, a magnetic null forms in the photosphere. Then, as the approach continues, the null rises into the corona and magnetic reconnection is driven there, which heats the bright point and can drive an x-ray jet (Shibata, this workshop).

We set up a simple model for this process, developed a numerical experiement and also applied the model successfully to some specific bright points Parnell et al (1995). A remarkable NIXT image revealed the internal structure of many bright points. For example, one has the shape of the wings and body of a mythical Norwegian bird (Figure 9a). Below this bright point in the photosphere, we found four magnetic fragments, one large positive fragment surrounded by three smaller negative fragments, giving a complex magnetic structure (Figure 9b). As the central fragment moves relative to the other three, it drives reconnection and transfers flux across the separatrix surfaces from one lobe to the other. Remarkably, the field lines that have just been reconnected and are therefore hot have the shape of the wings and body of the bird. Clearly, we can learn many more details of this basic process of bright points created by driven reconnection (both converging or emerging) from SOHO (e.g. Bocchialini, this workshop).

4.2. Yohkoh Observations of Loops

What are the implications of recent observations from Yohkoh of coronal loops? (Tsuneta (1996); Acton (1997)). A key result is that coronal loops (both small and large) appear to be heated by two independent mechanisms:

(i) an impulsive time-dependent mechanism, probably reconnection;

(ii) A background diffusive mechanism that is steady.

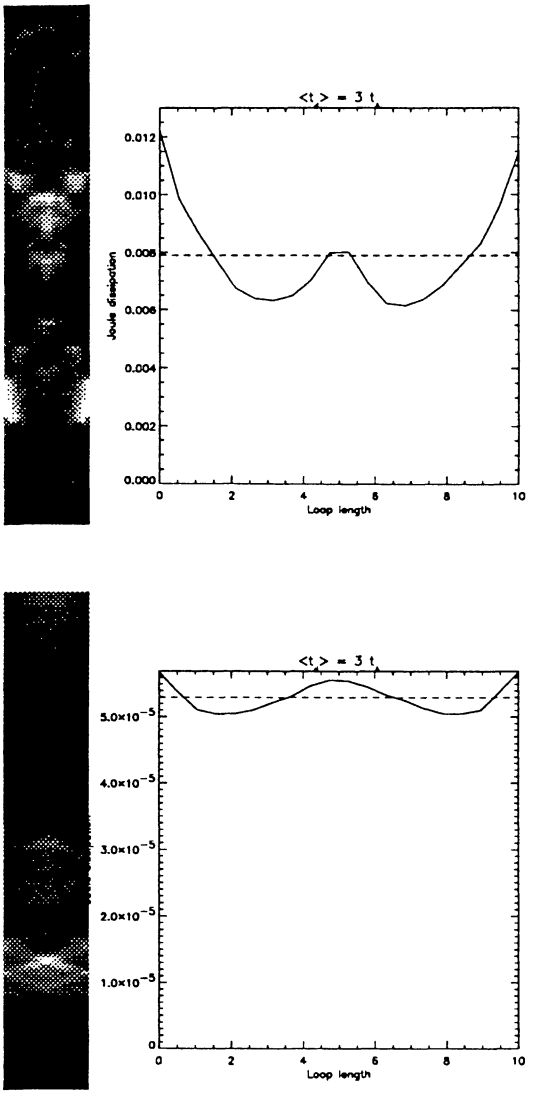

Figure 7. Joule dissipation as (a), (c) a function of position and time and (b), (d) averaged over time for rapid (top) and slow (bottom) driving.

The evidence for (i) is as follows. After large eruptions (coronal mass ejections) there are large rising cusps, produced by reconnection (Tsuneta (1992); Forbes & Acton (1996)). Also, large interconnecting loops are heated by reconnection as two active regions approach Tsuneta (1996). In addition many x-ray jets are a signature of reconnection (Shibata et al (1992)). Inside active regions one finds many transient brightenings (Schimizu et al (1992)). Also the loop temperatures lie between 2MK and 10MK (Yoshida & Tsuneta (1996); Kano, this workshop): short-lived loops (with lifetimes of a few hours or less) have high temperatures (6-7MK) and all the highest-temperature loops are either cusps or are multiple interacting loops, probably heated transiently by reconnection); longer-lived loops (a day or more) are cooler (2 - 4 MK) and are heated more steadily and uniformly.

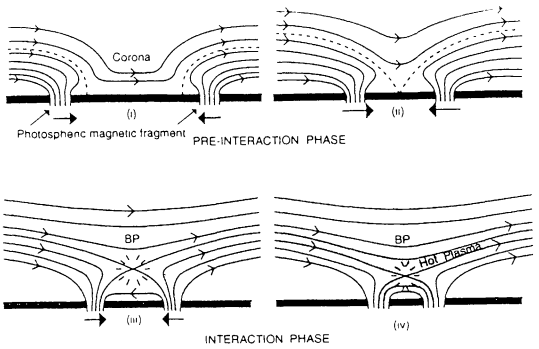

Figure 8. Converging flux model for an x-ray bright point

5. HEATING THE LARGE-SCALE DIFFUSE CORONA

How is the large-scale diffuse corona heated, which shows up as a beautiful halo of loops in Yohkoh SXT images? Is it simply a remnant of the heat liberated low down in the corona and conducted outwards? One of the paradigms about coronal heating is the belief that the overall or summit temperature of a loop is completely insensitive to the nature of the heating mechanism. This depressed many theorists, making them feel it would be impossible to unravel this secret of the Sun and discouraging them from comparing with observations. However, we have just realised that the temperature profile along a loop is highly sensitive to the nature of the heating. We have used Yohkoh SXT observations to measure the temperature along a large loop and have compared with a series of models and have deduced the likely form of the heating (Priest et al (1997)).

The simple coronal loop models that we have set up are as follows. Consider the part of the loop above 10^6 K where the radiation is negligible so that there is a balance

$$\frac{1}{A(s)}\frac{d}{ds}(A(s)\kappa_0 T^{5/2}\frac{dT}{ds}) = -H(s) \qquad (14)$$

between conduction and a heating (H) that depends on distance (s) along the loop from a footpoint ($s = 0$) where $T = T_0$ to the summit ($s = L$) where $dT/ds = 0$. Integrating (14) gives the heat flux

$$F(s) = -\kappa_0 T^{5/2}\frac{dT}{ds} = -\frac{1}{A(s)}\int_s^L HA\,ds \qquad (15)$$

and then integrating again gives the temperature profile ($T(s)$) as

$$T = T_0\left\{1 + \int_0^s \frac{7}{2\kappa_0 A T_0^{7/2}}ds' \int_{s'}^L HA ds''\right\}^{2/7}. \qquad (16)$$

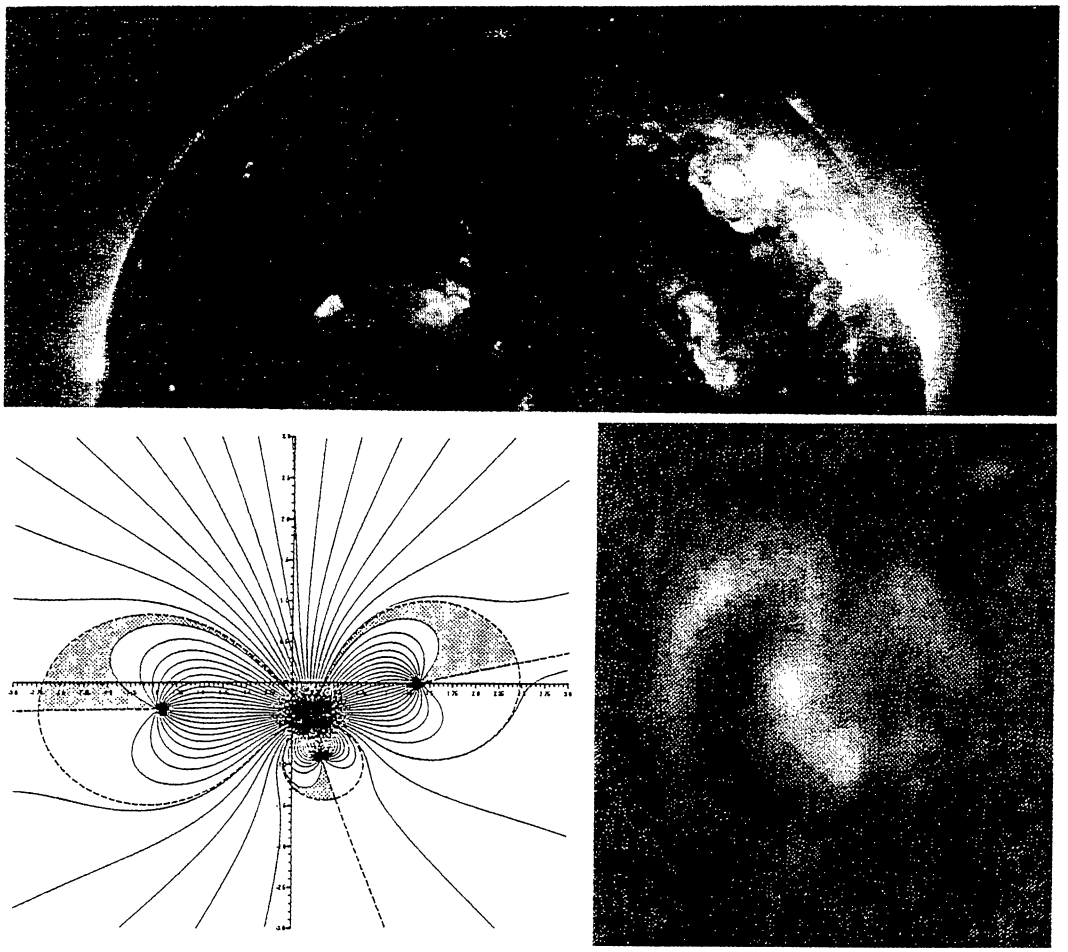

Figure 9. (a) Part of a full-disc NIXT image. (b) A close up of one of the bright points. (c) The corresponding magnetic field structure.

Assume now that the cross-sectional area (A) is constant, as is often observed, and consider the effect of different forms of heating (H). Suppose first that the heating is uniform along the loop ($H(s) = H_0$). Then the heat flux

$$-F = H_0(L - s) \tag{17}$$

is a linear function of s decreasing from $H_0 L$ to zero and

$$T^{7/2} = T_0^{7/2}\left(1 + \overline{H}\frac{Ls - \frac{1}{2}s^2}{L^2}\right) \tag{18}$$

is a quadratic function, where $\overline{H} = 7H_0L^2/(2\kappa_0 T_0^{7/2})$ is a heating parameter, (Figure 10, solid curves). By contrast, if H is uniform near the base and zero above it, then near the summit the heat flux is reduced to zero and the $T^{7/2}$ profile is flattened (Figure 10, dashed curves). Again, if H is uniform near the summit, then at low heights the heat flux is flattened and $T^{7/2}$ is linear (Figure 10, dotted curves). Similar conclusions hold if the heating has an exponential decrease from base or summit.

A Yohkoh full disc image is shown in Figure 11 (top), with a large-scale diffuse loop on the top right limb. We have measured the temperature ($T_{\rm obs}$) along this loop and compared with the above models. The most likely values of the parameters of the models (such as the magnitude of the heating) were determined by minimising

$$\chi^2 = \sum_i \frac{(T_{\rm obs} - T_{\rm model})^2}{\sigma_i^2},$$

where σ_i is the rms error in $T_{\rm obs}$ at distance s_i. χ^2/n, where n is the number of degrees of freedom, then has expected value 1 if the true model has been identified. Figure 11 (middle) shows how the observed temperature rises from 1.4 MK at one footpoint up to about 2.2 MK at the summit and then down to the other footpoint. A heating that is concentrated within 0.1L of the feet (top panel) gives a flat profile with a very poor fit ($\chi^2/n = 5.4$ and the significance level is less than 0.1 %). A heating that is localised at the loop top gives a pointed profile with a fit that is better but still not good ($\chi^2/n = 1.7$, significance level 10 %). However, a heating that is uniform (bottom panel) gives a good fit (χ^2/n, significance level 50 %).

We have therefore been able to make strong deduc-

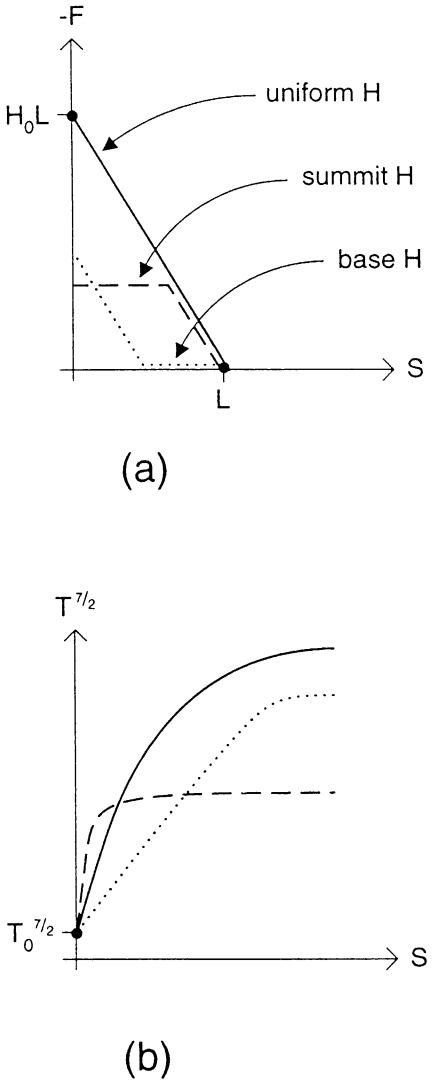

Figure 10. (a) Heat flux (F) and (b) temperature (T) as functions of distance (s) along a loop from foot ($s = 0$) to summit ($s = L$) for different forms of heating

tions about the form of the heating in a large diffuse loop. In particular, we have found the heating to be uniform rather than concentrated either at the loop feet or at the loop summit. In order to make the next step and deduce the heating mechanism, we need to know the forms of heating produced by the different mechanisms. These have not yet been calculated and so we cannot take such a step with confidence. However, we can deduce that diffuse loops are heated in situ rather than just being a conductive response to low-lying heating near the feet or to reconnection heating at their summits. Alfvén waves dissipating by phase mixing or resonant absorption also tend to heat preferentially near loop summits, where the wave amplitude for the fundamental is largest. If a loop broadened substantially at its summit, braids would tend to accumulate there and so give enhanced heating at the summit. However, loops tend to have rather uniform cross-sections and so heating by braiding tends to be fairly uniform. The resulting stochastic or turbulent heating is there-

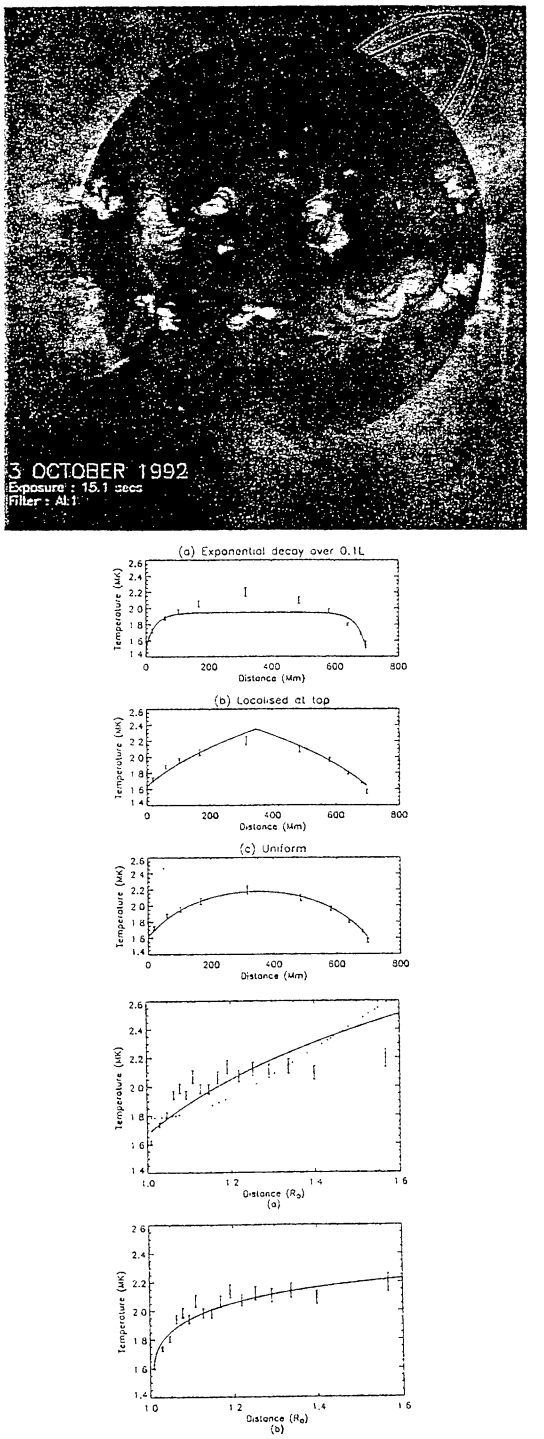

Figure 11. Yohkoh SXT image (top). Comparison of observed temperature along a large diffuse loop (middle three graphs). Comparison of observed temperature as a function of height in a large Yohkoh diffuse arcade (bottom two graphs) with models that have a flux that is (a) proportional to loop length (dotted), uniform (solid) and (b) proportional to the square of the magnetic field

We have also measured the temperature as a function

of height on the axis of the diffuse arcade and compared with models of an arcade of loops one above another, in each of which the temperature is given by the above loop models. But, if the heating is constant in each loop, we need to decide how that constant varies from one loop to another. Figure 12 shows the observed temperature profile. When the heating is uniform throughout the arcade the fit is very poor with a χ^2/n of only 5.0. If instead the heat flux at the base ($-F_0 = H_0 L$) is constant so that the heat per unit volume is less for the longer loops, then the fit is better ($\chi^2/n = 1.8$). However, if the heat in each loop scales with the square of the magnetic field and the arcade is modelled as a potential field with circular field lines, the fit is excellent ($\chi^2/n = 0.5$ with a significance level of 94 %).

6. CONCLUSION

First of all, we suggest that the amount of heat required in different coronal structures be reassessed and the variation of the turbulent velocity with height be studied in depth. In addition, it would be interesting to use SOHO to determine why some loops have a higher pressure than others.

The fact that the temperature profile along a loop and in an arcade is highly sensitive to the form of the heating opens a new door to try and determine the heating mechanism. In turn this is a stimulus to theorists to deduce the form of the heating produced by their favourite heating mechanism and to observers to refine their diagnostics and deduce the temperature profiles with as small an error as possible. This basic approach, which we have so far applied to large diffuse loops, can be applied the other types of loops and coronal structures which may well be heated by quite different heating mechanisms (Kano, Landi and Landini, at this workshop).

Finally, of course, there are many observations of other signatures which are being reported at this workshop. They include work on: Doppler shifts by Brekke, Brynildsen, Frevik, Kjeldseth-Moe, Lemaire; magnetic waves by Erdelyi, Fleck, Ofman; intensity and velocity variations by Ireland, Walsh, Hansteen, Wikstol; jets by Shibata, Curdt; and nanoflares by Judge. It is the complementary power of all these approaches which is likely to entice the Sun to reveal the many ways in which the corona is heated.

ACKNOWLEDGMENTS

I am delighted to acknowledge helpful discussions with St Andrews colleagues and financial support from the UK Particle Physics and Astronomy Research Council.

REFERENCES

Acton, L.W. 1997, Proc. Astron. Soc. Pacific, in press

Browning, P., Priest, E.R. 1984, A&A, 131, 283

Cally, P. 1991, J. Plasma Phys., 45, 453

Craig, I.J.D. Fabling, R.B. 1996, ApJ, 462, 969

Davila, J.M. 1987, Ap.J., 317, 514

Demoulin, P., Priest, E.R., Lonie, D.P. 1996, J. Geophys. Res., 101, 7631

Forbes, T., Acton, L.W. 1996, Ap.J., 459, 330

Galsgaard, K., Nordlund, A. 1996, JGR, 101, 13445

Galsgaard, K., Nordlund, A., Priest, E.R. 1997, in preparation

Goedbloed, J.P. 1975, Phys. Fluids, 15, 1090

Goossens, M. 1991, Advances in Solar System MHD (ed E.R. Priest and A.W. Hood) Cambridge, p137

Harvey, K.L. 1985, Aust J Phys., 38, 875

Heyvaerts, J., Priest, E.R. 1983, A&A, 117, 220

Heyvaerts, J., Priest, E.R. 1984, A&A, 137, 63

Heyvaerts, J., Priest, E.R. 1993, ApJ, 390, 297

Hollweg, J.V. 1984, ApJ, 277, 392

Inverarity, G., Priest, E.R., Heyvaerts, J. 1995, A&A, 293, 913

Jiao, L., McClymont, A.N., Mikic, Z. 1997, Solar Phys., in press

Litwin, C., Rosner, R. 1997, ApJ, in press

Mason, H. 1991, Proc 6th European Meeting on Solar Phys., p232

Mikic, Z., Schnack, D., Van Hoven, G. 1990 ApJ, 361, 690

Parker, E.N. 1972, ApJ, 174, 499

Parnell, C., Priest, E.R. 1995, Geophys. Astrophys. Fluid Dynamics, 80, 255

Parnell, C.E., Smith, J., Neukirch, T., Priest, E.R. 1996, Phys. of Plasmas, 3, 759

Priest, E.R., Parnell, C.E., Martin, S.F. 1994, ApJ, 427, 459

Priest, E.R., Demoulin, P. 1995, J. Geophys. Res., 100, 23,443

Priest, E.R., Titov, V.S. 1996, Phil. Trans. R. Soc. Lond. A., 354, 2951

Priest, E.R., Foley, C.R., Heyvaerts, J., Arber, T., Culhane, J.L., Acton, L.W. 1997, in preparation

Shibata, K., Ishido, Y., Acton, L., Strong, K., Hirayama, T., Uchida, Y., McAllister, A., Matsumoto, R., Tsuneta, S., Shimizu, T., Hara, H., Sakurai, T., Ichimoto, K., Nishino, Y., Ogawara, Y. 1992, Pub. Astron. Soc. Japan, 44, L173

Shimizu, T., Tsuneta, S., Acton L.W., Lemen, J.R., Uchida, Y. 1992, Pub Astron. Soc. Japan, 44, L147

Schindler, K., Hesse, M., Birn, J. 1988, J. Geophys. Res., 93, 5547

Tsuneta, S., Lemen, J.R. 1993, in Advances in Stellar and Solar Coronal Physics, (ed. J.K. Linsky and S. Serio) p113

Tsuneta, S. 1996, ApJ, 456, L63

Van Ballegooijen, A.A., 1986, Astrophys. J., 311, 1001

Yoshida, T., Tsuneta, S, 1996, ApJ, 459, 342